# Physical, Mechanical and Chemical Properties of nanocellulose Fibre Reinforced Mortar.

AGUNBIADE, Taiwo and MANGAT, Pritpal <http://orcid.org/0000-0003-1736-8891>

**Taiwo Agunbiade[1], P.S Mangat[2]**
*[1]Centre for Infrastructure Management, Materials and Engineering Research Institute, Sheffield Hallam University, Sheffield S1 1WB, UK, ta0168@hallam.shu.ac.uk*
*[2]Centre for Infrastructure Management, Materials and Engineering Research Institute, Sheffield Hallam University, Sheffield S1 1WB, UK, p.s.mangat@shu.ac.uk*

# PHYSICAL, MECHANICAL AND CHEMICAL PROPERTIES OF NANOCELLULOSE FIBRE REINFORCED MORTAR

## ABSTRACT

The paper presents an experimental investigation to evaluate the potential use of a water-based nanocellulose fibre derived from wood pulp sourced from sustainably managed forests in the applications of cementitious materials. The effect of the fibrillated cellulose fibre and its water-based solution on the physical, mechanical, shrinkage, and pore properties of OPC (ordinary Portland cement) mortar was investigated. Xrd and *ft-ir* analyses were performed to evaluate oxide composition, hydration products, bond interactions and functional groups present in the hydration products of the mortar samples reinforced with cellulose fibre. The shrinkage crack prevention provided by the cellulose fibre reinforcement under long-term drying conditions was also evaluated. Cellulose fibres were added to the mortar mixes in increments from 0.15% to 1.5% by weight of mortar. Results from the investigation reveal that the addition of cellulose fibre into the mortar mixes has a significant effect on the rheology of the matrix. The addition of cellulose fibre into the mortar matrix results in less than 10% increase or reduction in flexural and compressive strength at fibre contents which produce a workable mix. Drying shrinkage data for the mortar mixes after 28 days show that cellulose fibre in small amounts reduces the drying shrinkage as observed for mixes with fibre content up to 0.45%. The differential cumulative pore volume curves produced by a mercury intrusion porosimeter show that the cellulose fibres in the mortar matrix affect the large capillary pore volume for all the mortar mixes. All mixes exhibit bimodal pore size distribution profiles. A optimum dosage of 0.45% CF resulted in minimum drying shrinkage and no cracking of the mortar.

Keywords: nano fibre; cellulose fibre; mortar; shrinkage cracking; properties

## 1. INTRODUCTION

Waste materials mostly from agriculture wastes, have recently gained interest and attention as fillers and additives in cementitious composites. These applications have attracted interest from both science and construction industries, because of the sustainable benefits offered by such wastes, in addition to their cost-effective and environment-friendly nature. Since ancient Chinese and Egyptian civilisation, cellulosic vegetable fibres have been used as reinforcement for inorganic matrices to improve their mechanical properties and rheological behaviour (Ardanuy et al. 2011). This concept of fibre incorporation into cement matrix is based on the adhesive bonding properties which exist between the fibre and mortar matrix (Chen and Lui, 2005), control of internal micro cracking, internal self-curing ability, and shrinkage reduction at 0.5%CF (Zaki, 2015). Some of the commonly used fibres such as steel fibres, organic synthetic fibres, carbon fibres and glass fibres for reinforcements in cementitious composites exhibit advantages, such as long application time, relatively mature technology, and interesting physical and mechanical properties. However, compared to Cellulose fibres (CFs), these commonly used fibres have their limitations (Pandey et al. 2020). Steel fibres for example have high susceptibility to corrosion, relatively large density and as such may not be a choice of reinforcement for lightweight cementitious composites. Also, steel fibres lack the ability to induce growth of the hydrate gel in the cement matrix interface transition zone (Jie and Chun, 2021). Organic synthetic fibres are not biodegradable and exhibit poor compatibility and dispersion in cement matrix thereby resulting in compressive strength reduction (Kuruvilla et al. 2021). On the other hand, glass fibres are not susceptible to corrosion and are a good choice of reinforcement for manufacturing lightweight cementitious composites. However, their poor wear resistance and vulnerability in long-term alkaline environment (Kuruvilla et al. 2021) make them less desired reinforcement materials for specific applications in an alkaline environment. Carbon fibre is easy to agglomerate in the cement matrix, possesses long-term durability properties and good resistance to corrosion. Its major setback is the relatively high cost (Jie and Chun, 2021; Kuruvilla et al. 2021). Due to increasing demand for inexpensive environmentally friendly materials, and net zero goal of reducing the emission of greenhouse gases GHGs, researchers are making findings on the benefit of incorporating agricultural wastes in the form of processed fibres into cement mortars and concretes. Plant fibres are agricultural waste composed of cellulose, hemicellulose, lignin, and other substances used for application as reinforcement materials in cement and concrete. A recent study by Arbelaiz et al. (2023) investigated different cement-based composite properties reinforced with cellulose fibre. The composites were compared using the same variables and fabrication method after the addition of microfibers. The results indicated that the strength of mortar decreased compared with plain mortar, and the reduction was higher with increase in the fibre content. It was further observed that on addition of nanocellulose fibre, no change was observed in the density when compared with unreinforced mortar. Contrary to microfiber addition, the presence of 0.25% by weight nanocellulose in mortar slightly increased the flexural strength as reported by Arbelaiz et al. (2023). In another study by Mejdoub et al. (2017), nano-fibrillated oxidised cellulose (NFCox) in the range 0 -

1.5% by weight of cement was used as a cement paste partial replacement. According to the result, 0.7 wt.% of NFCox had the best outcome in lowering the thermal conductivity of the nanocomposite by 58% in comparison to the control sample's thermal conductivity value. The investigation further showed that by increasing the NFCox content, cement hydration increases as evident in the production of Ca $(OH)_2$ and C-S-H gel. These results were further supported by patterns from XRD and FTIR spectroscopy (D'Erme, Caseri and Santarelli, 2022). More studies have shown that the influence of fibrillated cellulose (FC) at dosages of 0%, 0.1%, 0.2% and 0.3 wt% by weight of binder on lime pastes and lime-based mortars enhances the flexural and compressive strengths respectively by 57% and 44% (D'Erme, Caseri and Santarelli, 2022). This current study aims to investigate the use of fibrillated cellulose fibre derived from wood pulp as a multifunctional additive in mortars.

## 2. MATERIALS AND METHODS

### 2.1. Materials and mixes

The Ordinary Portland Cement (OPC) conforming to CEM type 1 with a strength class of 32.5R used in this investigation was supplied by Frank-key Group, Sheffield. The sharp sand was supplied by WBB Minerals Ltd, Congleton, Cheshire. The gradation of the sand lies within the fine gradation zone (F Zone) specified in the British standard BS EN 882:2016 and ASTM C33. Table 1 shows the clinker phases obtained by Bogues calculation. The chemical analyses of the OPC and sand are shown in Table 2. The water used for the mixes conforms to the specifications in the British standard BS EN 1008:2002. The fibrillated cellulose fibre is derived from wood pulp that has been sourced from sustainably managed forests. The product is a multifunctional bio-based additive which can be used in concrete to provide unique rheological and physical properties. The cellulose fibre is supplied by Sappi Netherlands Services BV, Maastricht, Netherlands. The product specification and FT-IR spectra analysis are shown in Table 3 and Figure 1 respectively. The cellulose fibre was premixed with part of the mixing water at a Fibre content of 0.15wt %, 0.31wt%, 0.45wt%, 0.51wt%, and 1.5wt% of mortar. The mixture was homogenized by vigorously stirring at 1400 rpm/min at room temperature.

Commented [PM1]: Please check

Table 1. Chemical compositions of Type 1 OPC calculated from Bogues.

| Compounds | $C_3S$ (Alite) | $C_2S$ (Belite) | $C_3A$ | $C_4AF$ | $Al_2O_3$ | $CaCO_3$ |
|---|---|---|---|---|---|---|
| composition (mass %) | 31 | 38 | - | 4 | 2 | 24 |

Table 2. Chemical composition of Portland cement, sharp sand in (wt %).

| Oxides | $SiO_2$ | $Al_2O_3$ | $Fe_2O_3$ | CaO | MgO | $K_2O$ | $Na_2O$ | $TiO_2$ | $P_2O_5$ | MnO | $SO_3$ | LOI |
|---|---|---|---|---|---|---|---|---|---|---|---|---|
| **OPC** | 11.1 | 8.35 | 3.16 | 64.2 | 2.09 | 1.19 | 0.23 | 1.88 | 2.01 | 2.14 | 3.6 | - |
| **Sand** | 91.7 | 6.1 | 1.62 | 0.28 | 0.03 | - | 2.08 | - | - | - | 0.1 | 2.3 |

Specific gravity of OPC cement ($g/cm^3$): 3.15 [33],
Specific gravity of sharp sand ($g/cm^3$): 2.53 [33

Table 3. Product Specification of cellulose fibre

| Parameter | Value | Unit | Test method |
|---|---|---|---|
| Product form | paste | | Visual |
| Colour | White | % | Visual |
| Solid content | 9.0-11.0 | % | ESTM 9302 |
| Viscosity of 1.0% at 100 $s^{-1}$.20$^0$C | ≥600 | mPas | ESTM 5302 |
| pH of 1% suspension | 7.0-9.0 | | pH Meter |
| Total fines | ≥60 | % | ESTM 9003 |
| Preservative | Yes | | |

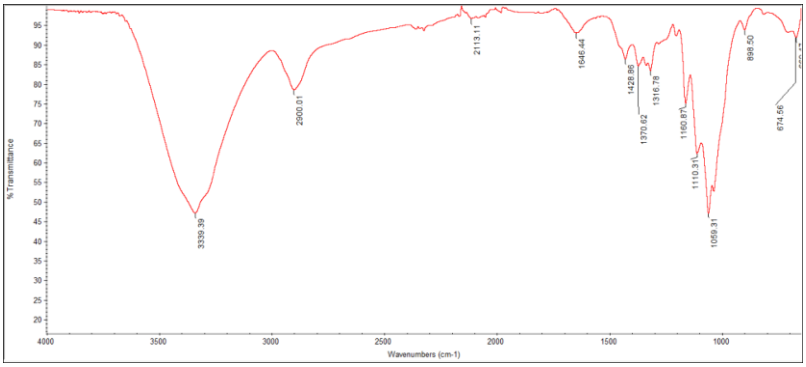


Figure 1. FT-IR spectra of cellulose fibre showing various functional groups.

Details of OPC control mortar and CFRM mixes are given in Table 4. Seven mixes of mortar (M0-M6) were investigated, M0 being the control mix comprising of Ordinary Portland cement and fine aggregates (sharp sand), M0-M6 mixes comprising the mortar matrix and cellulose fibre. The mortar mixes were based on a trial mix design for 40MPa, and they were investigated for compressive and flexural strength together with other properties.

Table 4. Mortar mix composition in (wt %)

| Mixes | CF content | Cement Content | Fine Aggregate (FA) | Water content | W/C |
|---|---|---|---|---|---|
| M0 | 0 | 19.6 | 68.6 | 11.8 | 0.59 |
| M1 | 0.15 | 19.6 | 68.6 | 11.8 | 0.59 |
| M2 | 0.31 | 19.6 | 68.6 | 11.8 | 0.59 |
| M3 | 0.45 | 19.6 | 68.6 | 11.8 | 0.59 |
| M4 | 0.51 | 19.6 | 68.6 | 11.8 | 0.59 |
| M5 | 0.99 | 19.6 | 68.6 | 11.8 | 0.59 |
| M6 | 1.5 | 19.6 | 68.6 | 11.8 | 0.59 |

Mix ratio Cement: FA (1:3.5)
CF content by weight of mortar ($M_1$-$M_6$: 0.15%, 0.31%, 0.45%, 0.51%, 0.99%, 1.5% respectively)

## 2.2. Specimen Preparation

### 2.2.1. Specimens for flexural, compression and drying shrinkage test

Flexural and compression test specimens of dimensions 160 x 40 x 40mm were prepared and cured in accordance with BS EN 1015-11. Shrinkage test specimens of same dimensions as specified in BS EN 1015-11 were cast and cured in the moulds at 65± 5% Relative Humidity (RH) and 20 ± $2^0$ for 24 hours. A total of twenty-one shrinkage test prisms were produced. After 24hrs the specimens were demoulded and demec discs were attached using epoxy along two longitudinal parallel (not the trowelled face) faces of each prism specimen at a gauge length of 100 mm. The samples were left for another 24 hours in the curing room before datum strain measurements were taken. Specimens were placed on a rack in the curing room with a clearance of at least 25 mm on all sides. A controlled temperature of 20 ± $2^0$C and 65± 5% RH was maintained in the curing room. Strain measurements were taken on the specimens at regular intervals with a DEMEC extensometer gauge at 65± 5% RH and 20 ± $2^0$C.

### 2.2.2. Specimens for Mercury Intrusion Porosimetry (MIP)

Selected mixes (M1, M2 and M3) were investigated based on the best compressive strength results obtained for the mixes. MIP test specimens between 2mm to 5mm were taken from the core of mortar specimens used for compression tests at the age of 28 days. The pieces of mortars were selected to avoid edges and skin effects due to mould, samples were kept in acetone for 24 hours, then dried for 1hr at 40ºC to remove the solvent. All samples were kept and stored in a polypropylene container prior to testing.

### 2.2.3. Specimens for XRD, XRF and FT-IR analysis

Pieces of mortars were obtained from broken compression test samples, ground into powder using a pulveriser and preserved in airtight polypropylene bags for xrd, xrf and ft-ir analysis.

## 2.3 Test Procedures

### 2.3.1 Workability, flexural and compressive strength

Flow test was performed in accordance with BS EN 1015-3:1999 to determine the workability of fresh mixes. The flexural strength of hardened mortar was tested by three-point loading of specimens to failure. Flexural tests were done on an Instron testing machine conforming to BS EN 12390-4:2019 at a constant loading rate of 30N/s. The compressive strength of the mortar was determined on two broken halves of test samples from the flexural strength test by a compression testing machine conforming to British standard BS EN 12390-4:2019, s at a constant loading rate of 0.3MPa/s.

### 2.3.2 Drying Shrinkage and Mercury Intrusion Porosimetry (MIP) Test

Drying shrinkage was measured using a mechanical strain gauge (DEMEC) which conforms to the standard BS 1881-206 with a gauge length of 100 mm. The DEMEC system directly measures the strain of the sample relative to an invar reference bar, with a resolution of 8 micro strains ($\mu\varepsilon$). The device measures the change in distance over time between two points on each side of the sample. *The MIP* test was conducted in accordance with BS ISO 15901-1:2016.

### 2.3.3 XRD and FTIR test

The powder samples of control mortar and CFRM were tested using a Philips X-Pert X-ray diffractometer operating with a Cu Kα radiation source (40 KV and 40 mA, wavelength λ = 0.154056 nm [6.07 × 10−9 in.]). XRD analysis of powder samples was performed by scanning from 5° to 100° at an angle of 2Θ; the scan step size was 0.016711 with a counting time step of 0.1 s. FTIR spectra were collected using a Nicolet FTIR spectrometer through the Attenuated total reflection (ATR) method. Spectra were recorded in the range of 500– 4000 $cm^{-1}$ with a 4 $cm^{-1}$ resolution and 32 co-added scans.

## 3.0. RESULTS AND DISCUSSION

### 3.1. Workability, flexural and compressive strength

#### 3.1.1. Workability

Figure 2 shows the flow curve of the control mortar and cellulose fibre-reinforced mortar (CFRM). The temperature of all the mixes lies between $23^0$C to $25^0$C except for mix 3 which is $18^0$C. It was observed that as the cellulose fibre content increases in the mixes, the workability (flow) reduces, resulting in stiff CFRM mixes M5 and M6. M0, M1, M2, and M3 showed good flow and were workable, spreadable, and easy for trowelling. M4 was moderately workable compared to M5 and M6. It was further observed that the cellulose fibres in the mortar mixes absorb large amount of the mixing water which led to a significant reduction in the consistency of the mixes from M0 to M6. This phenomenon has also been reported by (Sawsen et al. 2015; Buch et al. 1999).

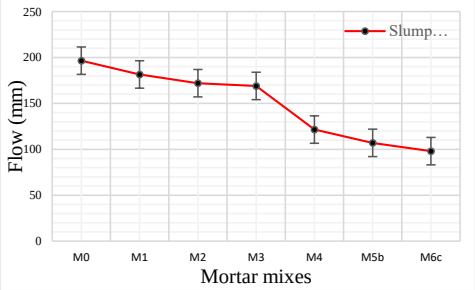


Figure 2. Flow curve of mortar mixes

### 3.1.2. Flexural Strength and Compressive Strength

Figure 3. and 4 illustrates the effect of cellulose fibres on the mortar flexural and compressive strength after 28 days of curing in water. The control mortar without CF gave 7.8Mpa flexural strength at 28 days, while mixes with CF content by weight of 0.15%, 0.31%, 0.45%, 0.51%, 0.99%, 1.5% gave 7.2Mpa, 7.5Mpa, 7.5Mpa, 7.2Mpa, 6.8Mpa, 5.3Mpa respectively. The results show that the flexural strength of the control mortar is greater than the CFRM samples. Mortar with cellulose fibre content of 0.31% and 0.45% gave the highest value of flexural strength but was lower than the control mortar without CF. Increasing the CF content incrementally beyond 1.5% results in a decrease in the flexural strength of mortar by 7.7%, 12.8% and 32% relative to the control. A similar trend was noticed for the compressive strength of the mortar mixes. As shown in figure 4.6, the mixes M1, M3, and M4 have minimal improvement in compressive strengths of 32.5Mpa, 32.6Mpa, and 34.2Mpa (7% increase) compared to the control mortar with 32Mpa. Mix M2, showed a slight decrease in compressive strength. CF contents beyond 0.51% result in a significant reduction in compressive strength by 9% (M5) and 29% (M6) compared to the control mortar (32Mpa). The fibre effect on the mechanical properties may be connected to the pore property changes caused by the fibres. This will be discussed in detail later.

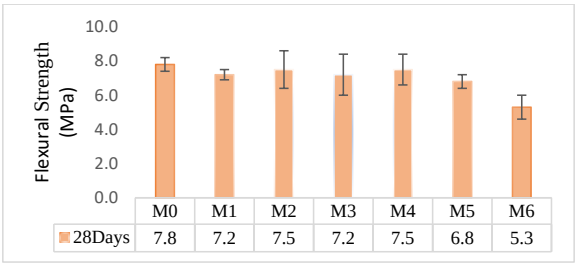


Figure 3. Flexural strength results of mortar mixes at 28 days after curing.

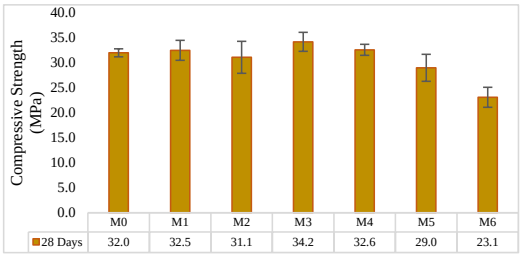


Figure 4. Compressive strength results of mortar mixes at 28 days after curing.

### 3.2. Drying shrinkage and surface cracking Test

Drying shrinkage was monitored for 30 days to observe the effect of CF on the mortar mixes. The results are shown in Figure 5. The control mortar mix M0 without cellulose fibre showed a drying shrinkage value of 780με. Mix M1 results in a reduction of drying shrinkage by 5% at 742με compared to the control mortar mix. M2 increased drying shrinkage by 5% at 816με, M3 (0.45% CF) resulted in 7% reduction in drying shrinkage at a strain value of 726με, M4, M5 and M6 all showed an increase in drying shrinkage by 6%, 16% and 19% with corresponding shrinkage value of 825με, 906με, and 925με respectively. After long curing exposure, the control mortar without CF and M3 with 0.45% CF were visually examined to evaluate the effect of CF on restraining surface cracking caused by drying shrinkage. Results shown in Figures 6a and 6b indicate that 0.45% CF prevents surface cracking compared to the control mortar which has significant surface cracking.

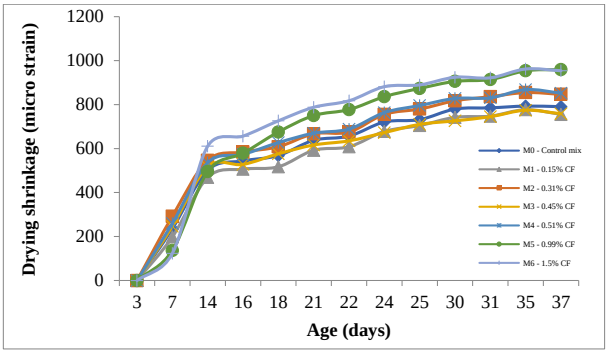


Figure 5. Drying shrinkage results of mortar mixes

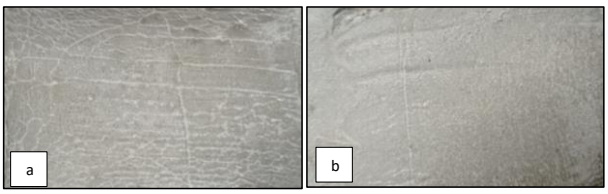


Figure 6a. Control mortar without CF; Figure 6b. Mortar with 0.45CF

### *3.3. Mercury Intrusion Porosimetry (MIP) test*

The Mercury Intrusion Porosimetry technique was used to investigate the total porosity of mortar mixes. The control mortar and three selected mixes (M1, M2, M3) were investigated. Results shown in Figures 7a and 7b from the experiment indicate that the ***total porosity*** of the control mortar mix M0 is approximately 19%. M1, M2, and M3 showed a total porosity of 25%, 27% and 24% respectively. The results indicate that

the incorporation of cellulose fibre into the OPC mortar mix significantly increased the porosity of the matrix.

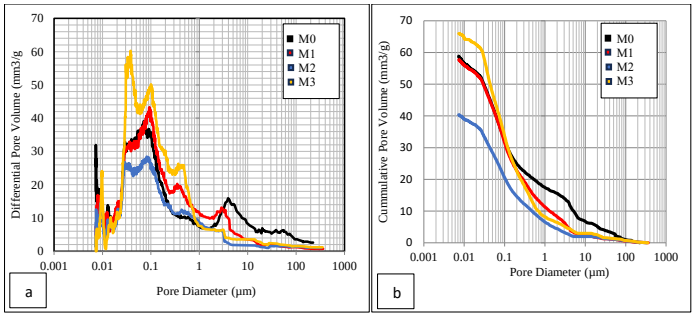


Figure 7(a) Differential pore volume curve for all mortar mixes; 7(b) cumulative pore volume curve for all mortar mixes.

### *3.4. Xrd and ft-ir test*

#### *3.4.1. XRD Analysis*

XRD analysis of mortar with different CF contents was investigated. The corresponding diffraction patterns after 28 days of curing are shown in Figures 8a, 8b, 8c. The hydration products for each mix are summarised in Table 8. The XRD patterns of all mixes with CF showed similar hydration products of portlandite ($Ca(OH)_2$ and calcium carbonate ($CaCO_3$), unreacted alites ($C_3S$) and belites ($C_2S$). These hydration products are not different from the control mortar. Similar hydration products have been reported by (D'Erme, Caseri and Santarelli, 2022; Mejdoub et al. 2017). Thus, no new hydration product was formed by addition of CF. It was further observed that several overlapping peaks and patterns of the hydration products makes it difficult to analyse changes in the hydration products with the addition of CF. Some secondary hydration products such as goethite and Iron dialuminium oxide were also found.

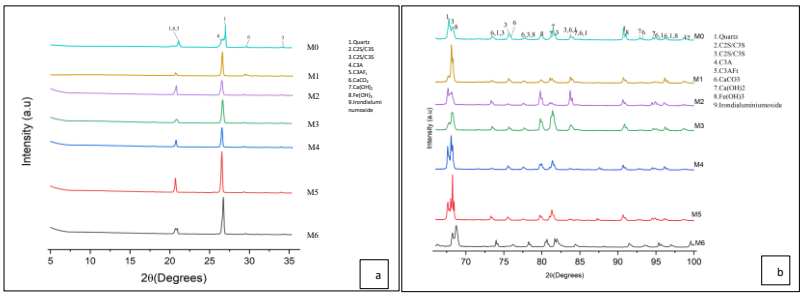


Figure 8a. xrd patterns of mortar mixes 5° -35°; Figure 8b. xrd patterns of mortar mixes 35° - 65°

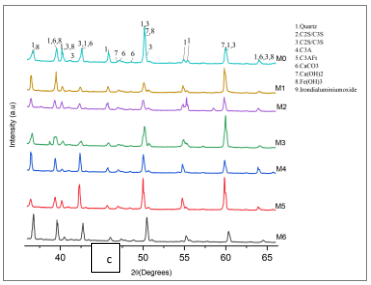


Figure 8c. XRD patterns of mortar mixes 65 º -100º

Table 5. XRD Quantification of hydration products of control mortar and CFRMs after 28 days of curing in wt %

| Mixes | Quartz | $C_3S$ | $C_2S$ | $CaCO_3$ | $Ca(OH)_2$ | $Fe(OH)_3$ | Iron di aluminium oxide |
|---|---|---|---|---|---|---|---|
| **M0** | 59 | - | 19 | 5 | 4 | 13 | - |
| **M1** | 82 | - | 7 | 4 | 1 | 5 | - |
| **M2** | 82 | 7 | - | 5 | 3 | - | 3 |
| **M3** | 88 | 7 | - | 3 | 2 | - | - |
| **M4** | 80 | - | 12 | 4 | 3 | - | - |
| **M5** | 93 | 4 | - | 2 | 1 | - | - |
| **M6** | 85 | - | 10 | 3 | 1 | 1 | - |

### *3.4.3 FT-IR Analysis*

Fourier transform infrared (FTIR) spectra of the control OPC mortar and CFRMs were analysed after 28 days of curing. Results in Figure 10a and 10b show a significant peak at about 3640 $cm^{-1}$ associated with O–H stretching vibrations of portlandite $(Ca(OH)_2$ in the control mortar. The Intensity reduces with the addition of CF with mix M1 having the weakest peak absorption at 3640 $cm^{-1}$ and the peak increases in M4, M2, M6, M5 and M3 respectively. This observation agrees with the XRD results for portlandite which reduces as Cellulose fibre is incorporated into the cement mortar matrix. The broad low peaks observed at about 3400 $cm^{-1}$ and 1641 cm-1 are usually associated with bound capillary water in calcium silicate hydrate colloidal gel-like structure. The peak (3400 $cm^{-1}$ and 1641 cm-1) shows a similar trend as observed for the band at 3640 $cm^{-1}$ in the case of portlandite. With the incorporation of cellulose fibre, a weak absorption band was observed for calcium silicate hydrate-bound water when compared to the control mortar without CF. The peaks observed at about 1415-1421 $cm^{-1}$ and 874 $cm^{-1}$ are associated with C-O and the presence of $CO_3$ bonds which indicate the presence of $CaCO_3$ (Herting and Odnevall 2021; Isokoski, Poteet, and Linnartz, 2013). It can be observed from the peaks that the control mortar has high presence of $CaCO_3$ and this calcite is reduced in intensity with an increase in CF content. This indicates that dosages 0.31% CF (M2), 0.51% CF (M4) and 0.15% CF (M1) promote the formation of $CaCO_3$ in the cement matrix which also suggests that

it may have contributed to the compressive strength of the mixes. Whereas at high CF dosages, mixes M5 and M6 exhibit lower peak absorption compared to the control mortar. The peaks at around 1030 $cm^{-1}$, 799, and 781 $cm^{-1}$ band region are assigned to Si-O crystalline structures of the mortar matrix. These observations indicate that CF addition promotes bond interactions between the OH functional groups and Si-O which results in slowing the hydration reaction of the matrix.

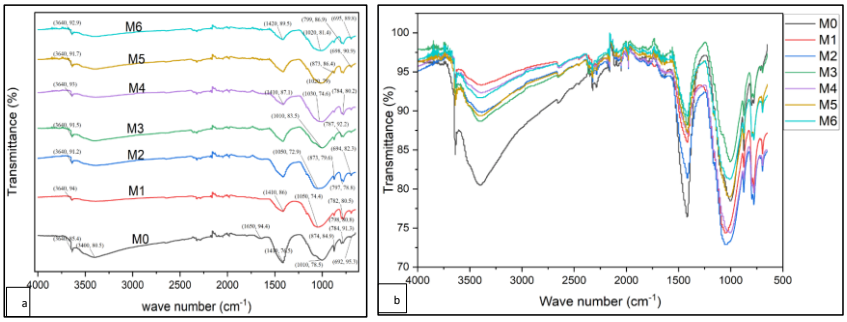


Figure 10. FTIR spectra of the M0, M1, M2, M3, M4, M5 and M6 mixes after 28 days of curing.

## 4. CONCLUSIONS

The following conclusions can be drawn from the study on the effect of cellulose fibre on OPC mortars:

The incorporation of cellulose fibre into the mortar matrix decreases workability as the amount of CF increases in the mix. As the CF content increases, the 28-day flexural strength reduces. The compressive strength of mortar at 28 days marginally increases with CF weight of 1.6%, 1.9%, and 6.8% but significantly reduces at CF dosage over 0.99% CF. Incorporation of CF at 0.15% and 0.45% into the mortar matrix results in lower drying shrinkage than the control mortar while higher dosages cause a marginal rise in the drying shrinkage than the control mortar. Cellulose fibre content of 0.45% causes very significant surface shrinkage crack reduction in the mortar as compared to the control mortar without CF. The cellulose fibres in the mortar matrix result in larger pore size formation thereby making the mortar matrix more porous compared to the control mortar without CF. The Xrd and ft-ir analysis show that, in the presence of CF, fewer hydration products with unreacted alites and belites were formed at 28 days age of curing. This suggests that the hydrophilic cellulose fibre absorbs a high volume of mixing water that could have contributed to the hydration process thereby delaying the degree of hydration and low hydration product formation. This phenomenon could benefit long-term durability and strength development by the gradual release of the absorbed water in the fibres for continuous hydration of the alites and belites.

**REFERENCES**


Arbelaiz, A., Ibarbia, J., Imaz, B. and Soto, L., 2023. Natural Fiber–Reinforced Cement Mortar Composite Physicomechanical Properties: From Cellulose Microfibers to Nanocellulose. *Journal of Materials in Civil Engineering*, *35*(5), p.04023094.

Ardanuy, Mònica & Claramunt, Josep & García-Hortal, José & Barra Bizinotto, Marilda. (2011). Fiber-matrix interactions in cement mortar composites reinforced with cellulosic fibers. Cellulose. 18. 281-289. 10.1007/s10570-011-9493-3.

BS 1881-206:1986 Testing concrete Recommendations for determination of strain in concrete

BS 812-103.2:1989 Testing aggregates. Method for determination of particle size distribution. Sedimentation test View details

BS EN 1008:2002 Mixing water for concrete - Specification for sampling, testing and assessing the suitability of water, including water recovered from processes in the concrete industry, as mixing water for concrete

BS EN 1015-3:1999 Methods of test for mortar for masonry. Determination of consistency of fresh mortar (by flow table)

BS EN 12390-4:2019 Testing hardened concrete. Compressive strength. Specification for testing machines

BS EN 12620:2002+A1:2008 Aggregates for concrete

BS EN 882:2016 Chemicals used for the treatment of water intended for human consumption. Sodium aluminate

BS ISO 15901-1:2016; Evaluation of pore size distribution and porosity of solid materials by mercury porosimetry and gas adsorption.

Buch, Neeraj & Rehman, Owais & Hiller, Jacob. (1999). Impact of Processed Cellulose Fibers on Portland Cement Concrete Properties. Transportation Research Record. 1668. 72-80. 10.3141/1668-11.

Chen, W.F., & Lui, E.M. (Eds.). (2005). Handbook of Structural Engineering (2nd ed.). CRC Press. https://doi.org/10.1201/9781420039931

D.Winslow and D. Liu, “The pore structure of paste in concrete,” Cement and Concrete Research, vol. 20, no. 2, pp. 227–235, 1990.

D’Erme C, Caseri WR, Santarelli ML. Effect of Fibrillated Cellulose on Lime Pastes and Mortars. *Materials*. 2022; 15(2):459. https://doi.org/10.3390/ma15020459

Gunasekaran, K.; Annadurai, R.; Kumar, P. Plastic shrinkage and deflection characteristics of coconut shell concrete slab. Constr. Build. Mater. 2013, 43, 203–207. [CrossRef]

Haitao Zhao, Qi Xiao, Donghui Huang, Shiping Zhang, "Influence of Pore Structure on Compressive Strength of Cement Mortar", The Scientific World Journal, vol. 2014, Article ID 247058, 12 pages, 2014. https://doi.org/10.1155/2014/247058

Herting, G.; Odnevall, I. Corrosion of Aluminium and Zinc in Concrete at Simulated Conditions of the Repository of Low Active Waste in Sweden. Corros. Mater. Degrad. 2021, 2, 150–162. [CrossRef] [32]

Isokoski, K.; Poteet, C.A.; Linnartz, H. Highly resolved infrared spectra of pure CO2ice (15–75 K). Astron. Astrophys. 2013, 555, A85. [CrossRef] [33]
Jie Liu, Chun Lv, "Research Progress on Durability of Cellulose Fiber-Reinforced Cement-Based Composites", *International Journal of Polymer Science*, vol. 2021, Article ID 1014531, 13 pages, 2021. https://doi.org/10.1155/2021/1014531
K. Pandey, T. Pal, R. Sharma, and K. K. Kar, “Study of matrix–filler interaction through correlations between structural and viscoelastic properties of carbonous-filler/polymer- matrix composites,” Journal of Applied Polymer Science, vol. 137, no. 27, pp. 48660–48660, 2020.
Kuruvilla, J.; Oksman, K.; Gejo, G.; Wilson, R.; Appukuttan, S. *Fiber Reinforced Composites: Constituents, Compatibility, Perspectives and Applications*; Woodhead Publishing: Cambridge, UK, 2021. [Google Scholar]

Luna, F. & Pérez, Álvaro & Alonso, M. (2018). The influence of curing and aging on chloride transport through ternary blended cement concrete. Materiales de Construcción. 68. 171. 10.3989/mc.2018.11917
Ma, Hongyan. (2014). Mercury intrusion porosimetry in concrete technology: Tips in measurement, pore structure parameter acquisition and application. Journal of Porous Materials. 21. 207-215. 10.1007/s10934-013-9765-4.
Mejdoub R, Hammi H, Suñol JJ, Khitouni M, M‘nif A, Boufi S. Nanofibrillated cellulose as nanoreinforcement in Portland cement: Thermal, mechanical and microstructural properties. Journal of Composite Materials. 2017;51(17):2491-2503. doi:10.1177/0021998316672090
S. Mindess, D. Darwin, J.F. Young, Concrete, 2nd edn. (Prentice Hall, Upper Saddle River, 2003)
Sawsen, C.; Fouzia, K.; Mohamed, B.; Moussa, G. Effect of flax fibers treatments on the rheological and the mechanical behavior of a cement composite. Constr. Build. Mater. 2015, 79, 229–235.
X. D. Chen, S. X. Wu, and J. K. Zhou, "Influence of porosity on compressive and tensile strength of cement mortar," Construction and Building Materials, vol. 40, pp. 869-874, 2013.
Z. Liu, D. Winslow, Cem. Concr. Res. 25, 769 (1995)
Zaki, El-Saaid. (2015). Application of ultra cellulose fibre for the enhancement of the durability and shrinkage of cement pastes exposed to normal and aggressive curing conditions. Nanotechnologies in Construction: A Scientific Internet-Journal. 8. 121-142. 10.15828/2075-8545-2015-7-4-121-142.
Zhu, Jie & Zhang, Rui & Zhang, Yang & He, Fa. (2019). The fractal characteristics of pore size distribution in cement-based materials and its effect on gas permeability. Scientific Reports. 9. 10.1038/s41598-019-53828-5.